

1 **Supplementary Information**

2
3 **A Multimode Biosensor Based on Prussian Blue Nanoparticle Loaded with**
4 **Gold Nanoclusters for the Detection of Aflatoxin B1**

5
6 Zhaodi Fu¹, Juan Huang², Wei Wei¹, Zhihui Wu^{2*}, Xingbo Shi^{2*}

7 *1, Testing Technology Company of Changsha Research Institute of Mining and Metallurgy Co., Ltd., Changsha*

8 *410012, China*

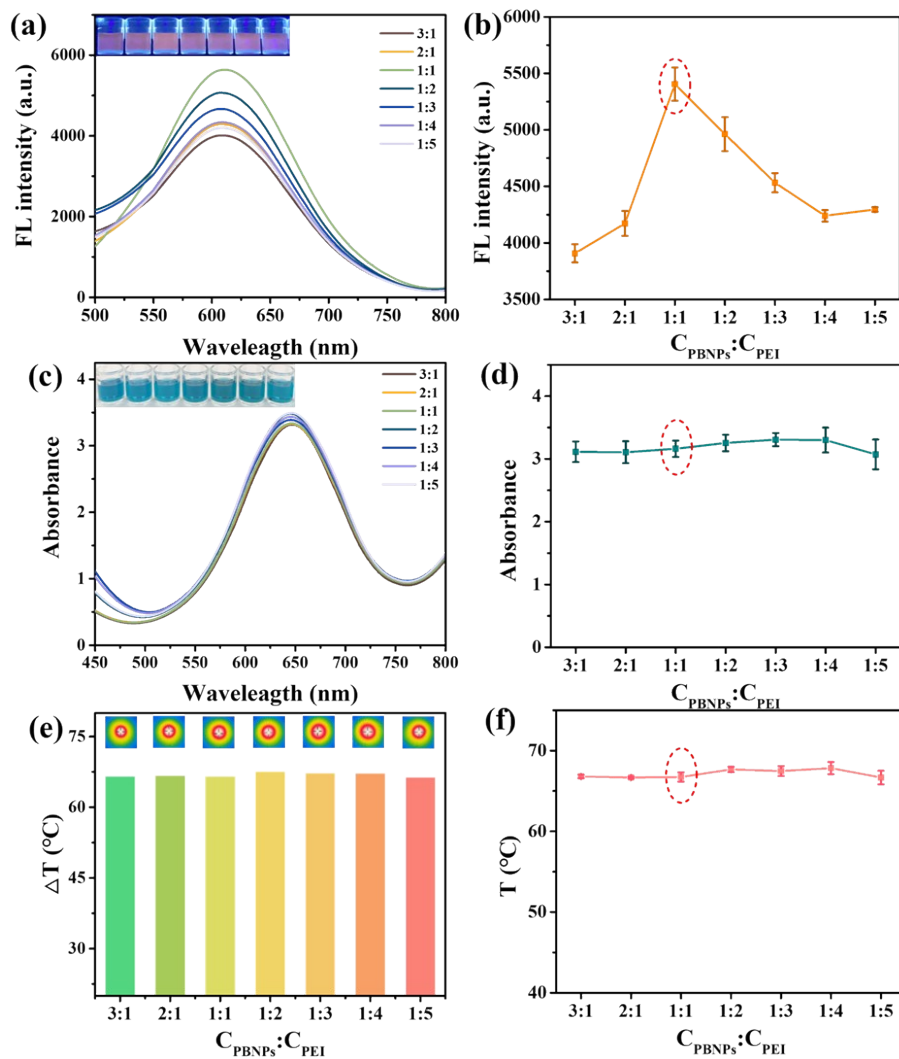
9 *2, Laboratory of Micro & Nano Biosensing Technology in Food Safety, Hunan Provincial Key Laboratory of Food*
10 *Science and Biotechnology, College of Food Science and Technology, Hunan Agricultural University, Changsha*

11 *410128, China*

12 ** Corresponding authors*

13 *E-mail address: wuzhihui@hunau.edu.cn; shixingbo123@hunau.edu.cn*

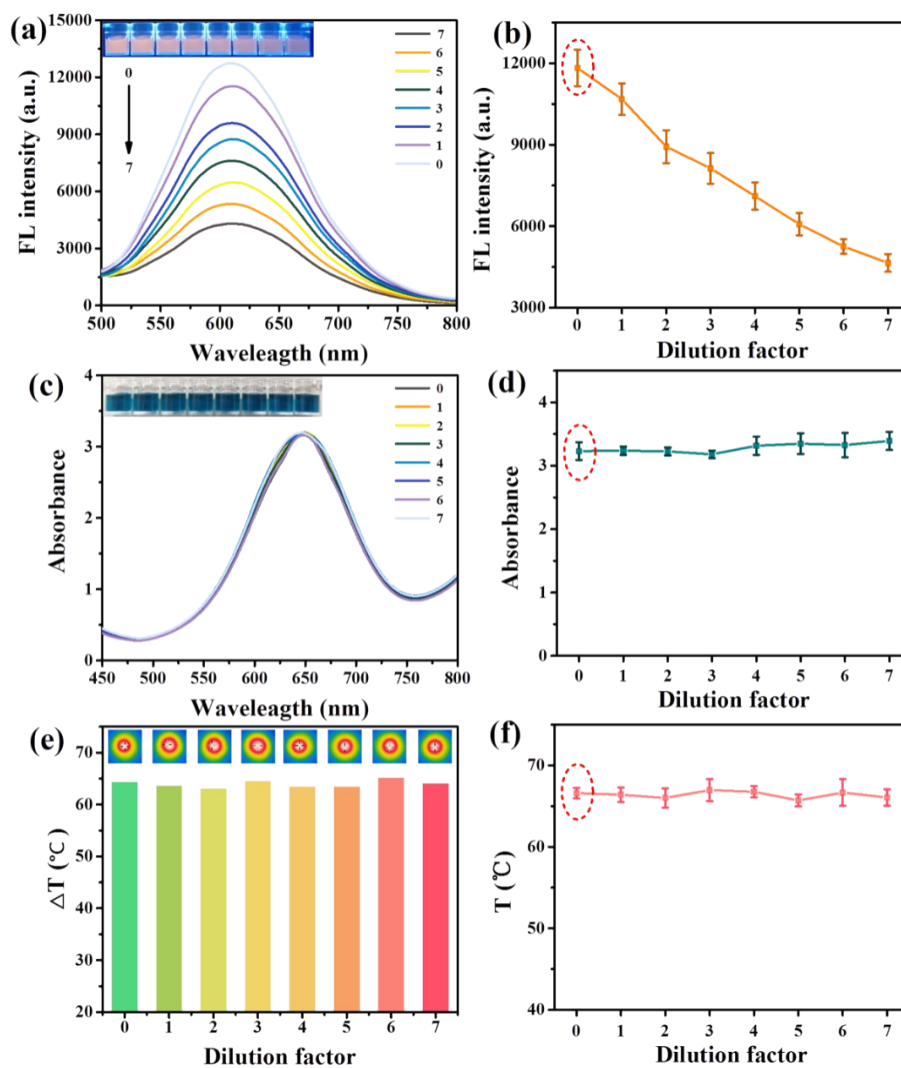
14



15

16

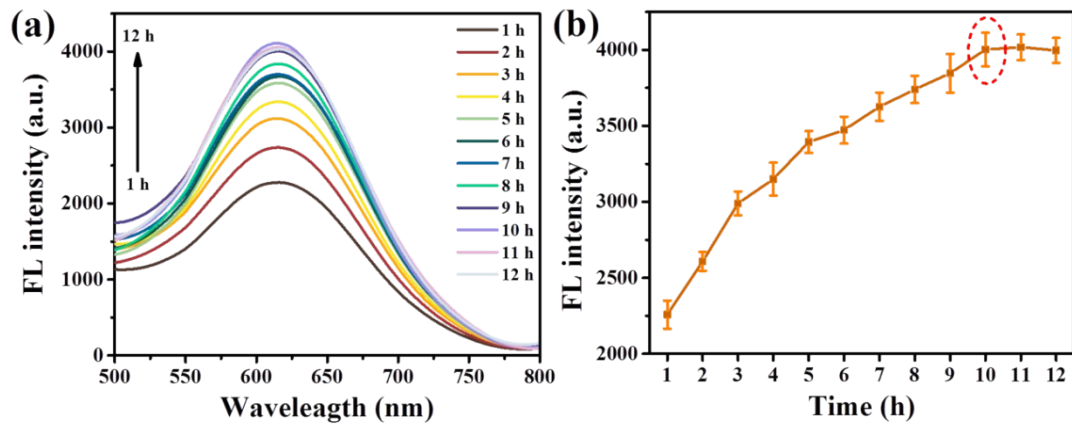
17 **Figure S1.** Optimization of preparation conditions for PBNPs-PEI@AuNCs. Changes in
 18 fluorescence values at 600 nm (a), UV-vis absorption values at 650 nm (c), and temperature values
 19 (e) of synthesized PBNPs-PEI@AuNCs when the ratio of PBNPs to PEI was 3:1, 2:1, 1:1, 1:2, 1:3,
 20 1:4 and 1:5, (b), (d) and (f) are corresponding optimized line charts.



21

22

23 **Figure S2.** Optimization of preparation conditions for PBNPs-PEI@AuNCs. Changes in
 24 fluorescence values at 600 nm (a), UV-vis absorption values at 650 nm (c) and temperature values (e)
 25 of synthesized PBNPs-PEI@AuNCs with different dilution factor (0, 1, 2, 3, 4, 5, 6 and 7) of AuNCs,
 26 (b), (d) and (f) are corresponding optimized line charts.



27

28

29 **Figure S3.** Optimization of preparation conditions for PBNPs-PEI@AuNCs. Changes in
 30 fluorescence values at 600 nm of PBNPs-PEI@AuNCs for AuNCs and PEI reaction times of 1, 2, 3,
 31 4, 5, 6, 7, 8, 9, 10, 11, and 12 h (a), (b) is corresponding optimized line charts.

32

33

34

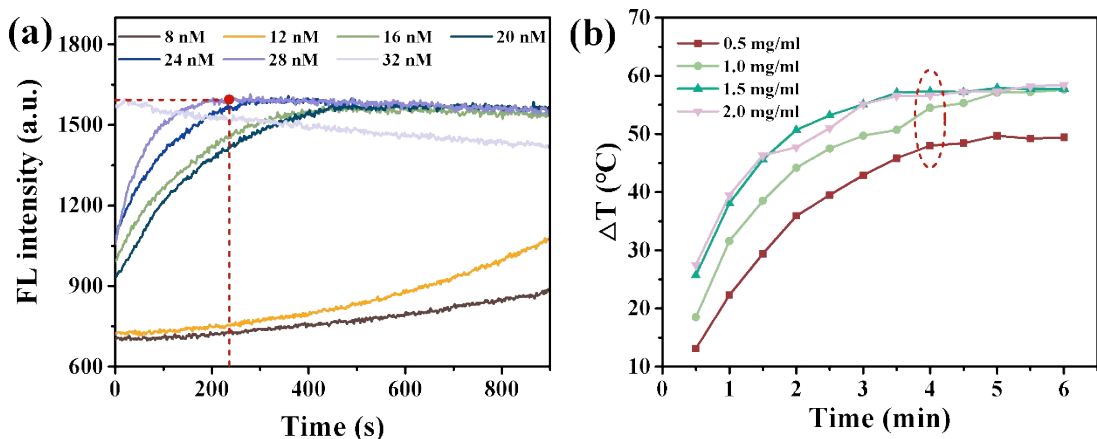
35

36

37

38

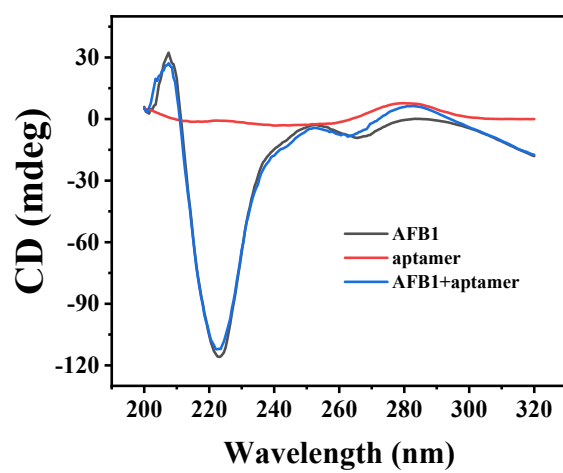
39



40
41

42 **Figure S4.** Optimization of preparation conditions for PBNPs-PEI@AuNCs. Fluorescence spectra of
 43 PBNPs-PEI@AuNCs solution increased with time after adding different concentrations (8, 12, 16, 20,
 44 24, 28, 32 nM) of NaOH solution (a). Heating curve of PBNPs-PEI@AuNCs solutions with different
 45 concentrations and increasing irradiation time (0.5, 1.0, 1.5, 2.0, 2.5, 3.0, 3.5, 4.0, 4.5, 5.0, 5.5, and
 46 6.0 min) of 808 nm excitation light (b).

47
48
49
50
51
52



53

54 **Figure S5.** CD spectra of AFB1, aptamers and complexes.

55

56

57

58

59

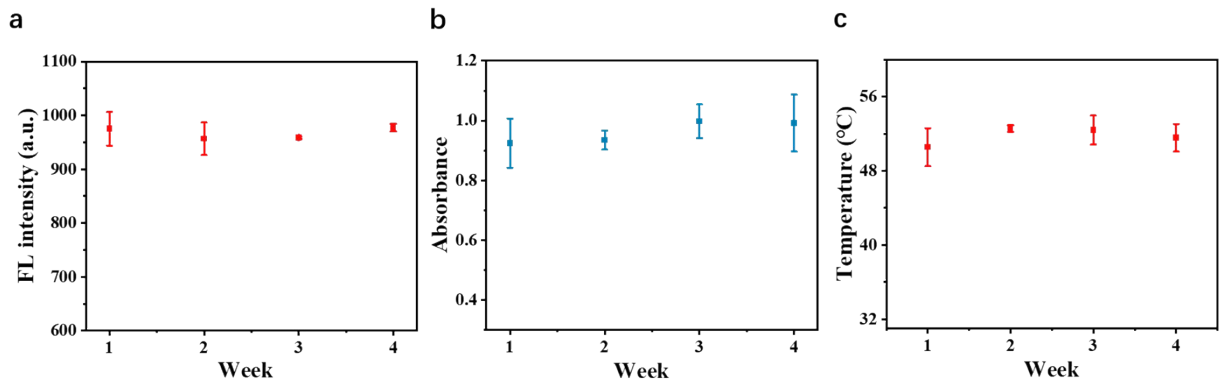
60

61

62

63

64



65

66 **Figure S6.** Evaluation the stability of the biosensor over a four-week period.

67

68

69

70

71

72

73

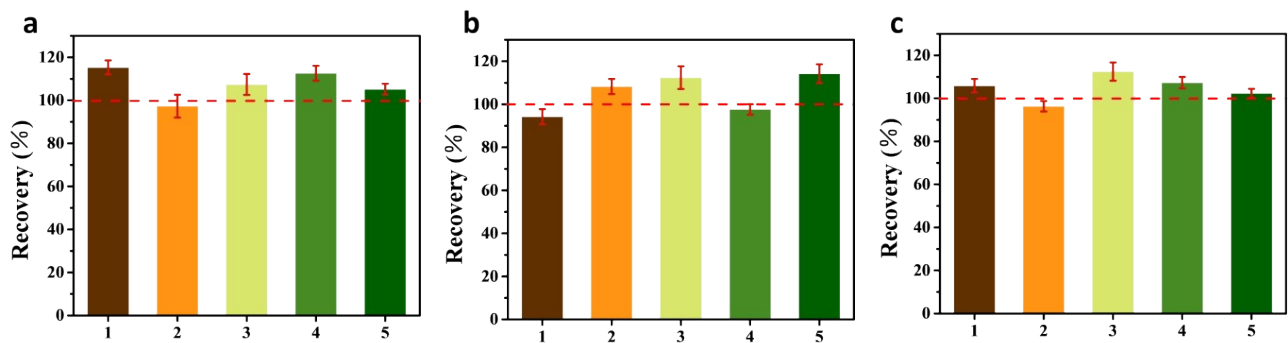
74

75

76

77

78



79

80

81 **Figure S7.** Recovery results for AFB1 detection using this strategy: fluorescence signal (a),
82 colorimetric signal (b), and temperature signal (c), the concentration of AFB1 in samples 1-5 was 10^{-14} , 10^{-13} , 10^{-12} , 10^{-11} , and 10^{-10} g/mL in sequence.

84

85

86

87

88

89

90

91 **Table S1.** Schematic diagram of the sensing strategy of multimode signal detection of AFB1 based on PBNPs-PEI@AuNCs.

Spiked (g/mL)	Fluorescent signal		Colorimetric signal		Photothermal signal	
	Found (g/mL)	RSD (%, n=3)	Found (g/mL)	RSD (%, n=3)	Found (g/mL)	RSD (%, n=3)
10 ⁻¹⁰	1.15 × 10 ⁻¹⁰	1.48	0.94 × 10 ⁻⁹	0.98	1.06 × 10 ⁻¹⁰	2.85
10 ⁻¹¹	9.73 × 10 ⁻¹⁰	0.49	1.08 × 10 ⁻¹¹	2.43	9.63 × 10 ⁻¹¹	0.24
10 ⁻¹²	1.07 × 10 ⁻¹²	0.24	1.12 × 10 ⁻¹²	1.45	1.12 × 10 ⁻¹²	3.48
10 ⁻¹³	1.13 × 10 ⁻¹³	1.70	0.98 × 10 ⁻¹²	0.65	1.07 × 10 ⁻¹³	1.48
10 ⁻¹⁴	1.05 × 10 ⁻¹⁴	0.95	1.14 × 10 ⁻¹⁴	0.38	1.02 × 10 ⁻¹⁴	0.57

92

93

94

95

96

97

98

99 **Table S2.** Result comparison of the sensing strategy and the commercial ELISA kits for the detection of AFB1 in food samples.

Samples	ELISA kit		Fluorescent Signal		Colorimetric Signal		Photothermal Signal	
	Detected ($\mu\text{g/kg}$)	RSD (%, n=3)	Detected ($\mu\text{g/kg}$)	RSD (%, n=3)	Detected ($\mu\text{g/kg}$)	RSD (%, n=3)	Detected ($\mu\text{g/kg}$)	RSD (%, n=3)
Cereal	Non	--	Non	--	Non	--	Non	--
Peanut	0.12	2.60	0.13	1.36	0.13	3.75	0.11	2.07
Biscuit	Non	--	2.43×10^{-3}	2.49	2.53×10^{-3}	4.49	2.31×10^{-3}	1.99

100